Available online at www.sciencedirect.com
ScienceDirect
Ceramics International 35 (2009) 2789–2795
CERAMICS INTERNATIONAL
www.elsevier.com/locate/ceramint

Characterization of basaltic tuffs and their applications for the production of ceramic and glass–ceramic materials

Sibel Ergul [a], Fabiola Ferrante [b], Paola Pisciella [b,*], Alexander Karamanov [c], Mario Pelino [b]

[a] Department of Structural, Water and Soil Engineering, University of L'Aquila, 67040 Monteluco di Roio – L'Aquila, Italy
[b] Department of Chemistry, Chemical Engineering and Materials, University of L'Aquila, 67040 Monteluco di Roio – L'Aquila, Italy
[c] Institute of Physical Chemistry, Bulgarian Academy of Sciences, Acad. G. Bonchev str. Bl.11, 1113 Sofia, Bulgaria

Received 18 August 2008; received in revised form 17 February 2009; accepted 14 March 2009
Available online 15 April 2009

Abstract

Alkaline basaltic tuffs, from Southern Turkey were characterized and employed to obtain ceramic and glass–ceramic materials by combined sintering and crystallization process. The chemical and mineralogical compositions were analyzed by X-ray fluorescence spectrometry and X-ray diffraction analyses, respectively. The phase formation and the sintering behaviour were investigated by DTA, differential dilatometer and hot-stage microscopy. The micro-structure and residual porosity of the sintered samples were observed by SEM and evaluated by pycnometric techniques. Ceramic material, based on 50% basaltic tuff and 50% clay, was obtained at 1150 °C with 13% total porosity and 4% water absorption. Glass–ceramic materials were synthesized directly using the milled basaltic tuff by mean of the sinter-crystallization technique, in the range 900–1150 °C. The investigation has showed that, due to the high porosity and low crystallinity, alkaline tuffs could be a suitable raw material for ceramic application.

Keywords: A. Sintering; B. Porosity; D. Traditional ceramics; D. Glass ceramics; Basaltic tuffs

1. Introduction

Presently, the raw material deposits, appropriate for the traditional ceramic industry, are restricted and their manufacturing expenses continuously increase. Therefore, many of the recent studies related to earthenware and porcelain stoneware compositions concerned the substitution of the traditional raw materials with other low-cost minerals or/and waste [1]. Some promising results were obtained using glass cullet [2–4], different industrial wastes [5–6] as well as some pyroclastic outcrops with acidic compositions as volcanic ash and zeolite rich rocks [7–9]. Other igneous rocks, whose properties could be suitable for the ceramic industry, are the alkaline basaltic tuff compositions. They show a high crystallization tendency and the compositions are characterized by low melting temperature and 2–3 wt% titanium and 10–14% of iron oxides content [10]. The occurrence of these oxides leads to a fast precipitation of titanium magnetite and to a spontaneous formation of a fine crystalline structure [11].

It is known that basaltic compositions or iron-rich silicates have been employed in the petrurgy (refused rock industry), to produce building tiles, pipes and bends and glassy insulation fibres [12]. Up to now, the petrurgical technology has mostly employed tholeiite basalts or diabasic rocks [13–15], which are characterized by a reduced tendency to spontaneous crystallization, due to their high viscosity. Basalt like glasses and glass ceramics have been also developed to encapsulate the nuclear waste before disposal and, more recently, for the vitrification of various hazardous industrial wastes [16–19].

The most common method to synthesize glass–ceramic materials is by heterogeneous nucleation, introducing insoluble crystallization nuclei into the bulk of the melt. In alternative the sinter-crystallization technique, allows the simultaneous sintering of the glass powders and the crystalline phase formation [20–22]. In this way it is possible to manufacture glass ceramics at low temperature and with short production cycles. Typical examples are the iron-rich silicate compositions [17,23–25]. Owing to low viscosity, alkaline basaltic tuffs with high amount of glassy phase appear appropriated for the

* Corresponding author. Tel.: +39 862 434224; fax: +39 862 434233.
E-mail address: pelino@ing.univaq.it (P. Pisciella).

0272-8842/$36.00 © 2009 Published by Elsevier Ltd and Techna Group S.r.l.
doi:10.1016/j.ceramint.2009.03.026

production of glass–ceramic materials by sinter-crystallization technique. It is supposed that this peculiarity might give the possibility to obtain sintered glass–ceramic materials by using only a sinter-crystallization heat-treatment.

The aim of the present work is the characterization of an alkaline–olivine basaltic tuff, from Southern Anatolia, and its application in the synthesis of the ceramic and glass–ceramic materials by using the combined sintering and crystallization technique.

2. Experimental

The alkaline–olivine basaltic tuffs were milled for 30 min in an agate mortar, using a Resch centrifugal mill, and then sieved below 75 μm. The obtained powder was observed by optical microscopy to estimate the particle shapes and dimensions.

Part of the basaltic tuff was melted for 30 min at 1350 °C and the melt was quenched in water. The resulting glass frit was milled and sieved below 75 μm. XRD analysis, carried out on the glass frit sample showed a completely amorphous structure.

Green ceramic samples (BC) were obtained by mixing 50 wt% tuffs, 30 wt% kaolinitic clays and 20% illitic clays. The batch was humidified with 8% water and uniaxially pressed at 30 MPa.

Glass–ceramic samples were obtained from the frit (BG) or from the basaltic tuff powders (BT), after pressing at 150 MPa using 7.5% polyvinyl alcohol solution as a binder.

The chemical analyses of the basaltic raw materials and the products were performed by XRF analysis (Spectro XEPOS). The results are shown in Table 1.

The thermal behaviour of the milled basaltic tuff (BT) and frit (BG) was investigated by DTA (Netzch STA 409), using 100 mg powder sample at a 10 °C/min heating rate.

The sintering behaviour of the ceramic (BC), glass frit (BG) and as it is basaltic tuff (BT) powders were evaluated at 10 °C/min heating rate by differential dilatometer (Netzsch 402 ED), using 10 mm × 4 mm × 4 mm "green" samples. Then, BT and BC 10 mm × 10 mm × 8 mm green samples were heat-treated at different temperatures in the range 900–1150 °C and the micro-structure was investigated by pycnometric techniques. The bulk (apparent) density, ρ_b, was measured by a dry flow pycnometer (GeoPyc 1360). The skeleton (relative), ρ_s, and real (absolute), ρ_r, densities were measured by He displacement Pycnometer (AccuPyc 1330) [26] before and after milling the samples below 53 μm, respectively. Density results were used to determine the total porosity, $P_T = 100 \times [(\rho_r - \rho_b)/\rho_r]$, closed porosity, $P_C = 100 \times [(\rho_r - \rho_s)/\rho_r]$ and open porosity, $P_O = P_T - P_C$.

The surface and fracture morphology of the final samples was observed by Scanning Electron Microscopy (SEM) after Au metallization.

The phase analysis of the raw materials and obtained sintered samples were carried out by XRD (Philips PW1830 apparatus and CuK_α radiation). The crystal phase fraction was estimated by comparing the total area of the crystalline phases with the amorphous halo in the XRD spectrum [21].

Table 1
Chemical compositions of the raw materials and batch (BC).

wt%	Basaltic tuffs	Illitic clay	Kaolinitic clay	BC
SiO_2	44.07 ± 0.07	52.50 ± 0.09	55.0 ± 0.08	51.0 ± 0.08
Al_2O_3	14.51 ± 0.04	25.12 ± 0.06	30.21 ± 0.06	18.5 ± 0.07
TiO_2	3.06 ± 0.01	0.72 ± 0.02	1.52 ± 0.03	2.00 ± 0.04
Fe_2O_3	14.04 ± 0.04	7.91 ± 0.03	0.55 ± 0.001	9.34 ± 0.03
CaO	9.92 ± 0.05	tr	0.29 ± 0.01	5.51 ± 0.02
MgO	7.87 ± 0.07	2.5 ± 0.05	0.73 ± 0.02	4.56 ± 0.08
Na_2O	4.12 ± 0.17	0.40 ± 0.02	3.26 ± 0.13	3.52 ± 0.04
K_2O	1.73 ± 0.01	4.3 ± 0.02	0.57 ± 0.01	2.19 ± 0.02

3. Results and discussion

3.1. Characterization of the raw materials

The chemical analyses of the investigated tuff are presented in Table 1 showing typical alkaline–olivine basalt compositions.

All samples contain 40–50% glass-forming oxides (i.e. $SiO_2 + Al_2O_3$), which should yield a good chemical resistance, as well as elevate percentages of CaO, MgO and Fe_2O_3, ensuring a high crystallization trend and formation of appropriated silicate and alumino-silicate crystalline phases. The trace elements are mainly Zr, Y and Nb with concentrations of 218.6, 26.1 and 57.93 ppm respectively and are also typical of alkaline basalt compositions (see Table 1). Fig. 1 shows the Winchester and Floyd Nb/Y–Zr/TiO_2 diagram highlighting the formation of the alkaline basaltic igneous rocks [27]. Fig. 2a shows a thin section of the tuff with prismatic bluish-green pyroxene minerals embedded in an amorphous matrix, high relief olivines with active yellow colours and felsic plagioclase microliters. The high amount of glassy phase is due to the tuff formation (i.e. intensive eruption, followed by fast water cooling). Tuffs are generally characterized by a 40–60% open porosity (Fig. 2b).

Due to the low crystallinity and high porosity the tuff employed in this study was easily crushed and milled. In fact,

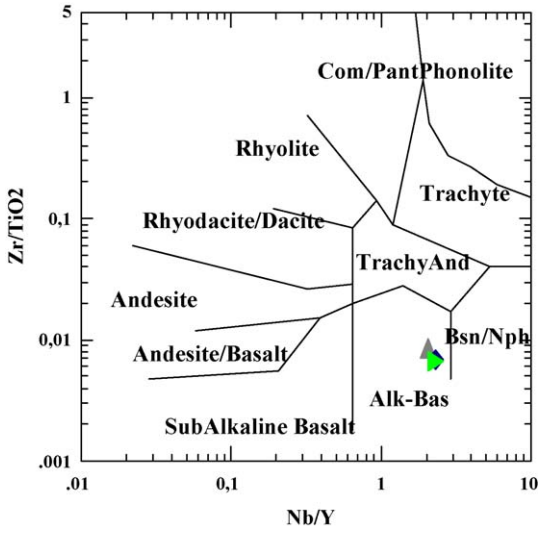

Fig. 1. Nb/Y–Zr/TiO_2 diagram highlighting the tuff composition.

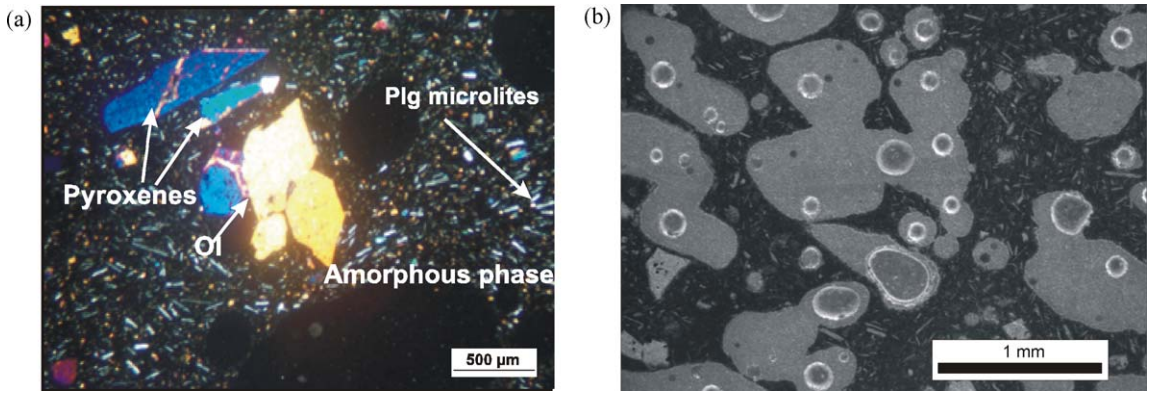

Fig. 2. (a) Optical microscopy of the tuff section. (b) Thin section microscopy of the tuff.

after 30 min milling, the powder showed a particle size ranges between 20 and 70 μm and a sub-angular and semi-spherical shapes. On the other hand, it is well known that the basaltic rocks formed by lava flow and slow cooling, are characterized by negligible porosity, high crystallinity and elevate hardness which generate difficulties during grinding and milling [28].

3.2. Sintering of ceramics and glass ceramics

In previous works it was demonstrated that the phase formation rate in the iron-rich compositions depends on the Fe^{2+}/Fe^{3+}ratio: the closer is this ratio to the magnetite ($FeO{\cdot}Fe_2O_3$) value of 0.5, the higher is the crystallization trend [12,15,16,23,29]. The Fe^{2+}/Fe^{3+}ratio also influences the sinter-crystallization of the glass powders [8,16,17,20]. In air atmosphere, the formation of magnetite spinels can be inhibited by the surface Fe^{2+} oxidation; the crystallization rate is proportionally reduced and at high temperature the formation of hematite (Fe_2O_3) takes place.

In Fig. 3 the DTA curves of BT and BG samples are reported. The Tg of BG occurs similarly to others at 650 °C, which is typical for iron-rich glass compositions [18,23,30,31]. As reported in other works, in iron-rich glasses, the surface oxidation of Fe^{2+} to yield Fe^{3+} leads to hematite formation on the surface [17,18,32] exerting a strong impact on the crystallization behaviour of the glass at high temperatures.

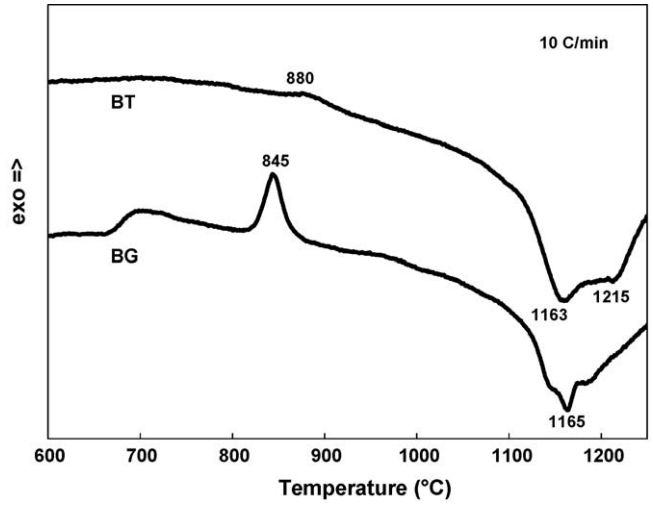

Fig. 3. DTA traces of the BT and BG samples.

The DTA curve of BG shows a strong crystallization effect at 845 °C due to the crystallization of the amorphous phase, an endothermic effect occurs at 1165 °C enhanced by the presence of TiO_2 in the parent tuff which acts as nucleating agent [33,12,21].

The DTA trace of BT sample shows a strong exothermic effect at 880 °C due to the crystallization of the glassy phase present in the tuff, followed by an intensive endothermic peak in the range 1100–1250 °C due to the melting of the crystalline phases. The BT crystallization occurs at higher temperature because of the higher apparent viscosity, due to the higher degree of crystallinity [34].

The dilatometric trace of BC highlights a ∼0.5% linear shrinkage in the range 980–1020 °C, due to the phase transformation of metakaolinite. At 1100 °C a permanent linear contraction takes place indicating the onset of the sintering and from 1185 °C, a strong densification rate is registered; the shrinkage attains a value of 13% at 1200 °C. The BC sintering behaviour, i.e. large contraction and high densification rate, suggests the formation of a liquid phase due the iron oxides content [35].

The dilatometric curve of BG, shows the beginning of sintering at 650 °C (i.e. in the glass-transition range) and a linear shrinkage ($\Delta L/Lo$) of about 8% at 880 °C. After 900 °C the densification is inhibited by the intensive crystal phase formation on the surface of the particles. Further densification is obtained only after 1020 °C and a complete sintering of the sample is reached at about 1100 °C (i.e. at 100 °C lower temperature than BC). The comparison of the DTA and dilatometric curves of BG, Figs. 3 and 4 respectively, indicates that the sintering at 1100 °C can be related to a partial melting of the formed crystalline phases.

In BT, the sintering starts at about 740 °C (i.e. about 90 °C higher than BG) and the densification rate is lower because of the high percentage of crystal phase. As a result, at 870 °C,

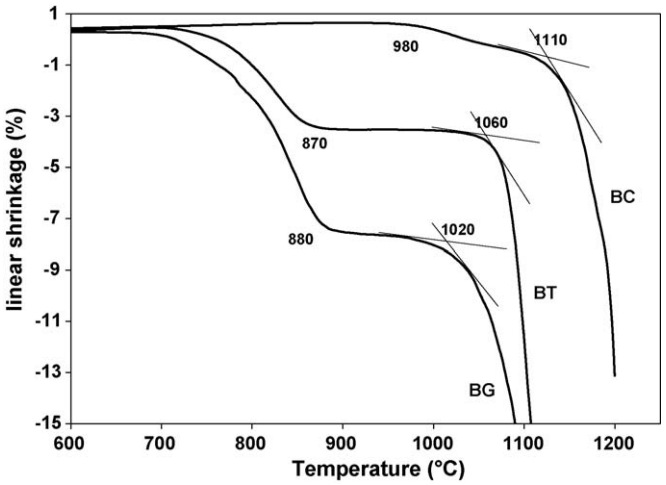

Fig. 4. Dilatometric traces of the BT, BG, BC samples.

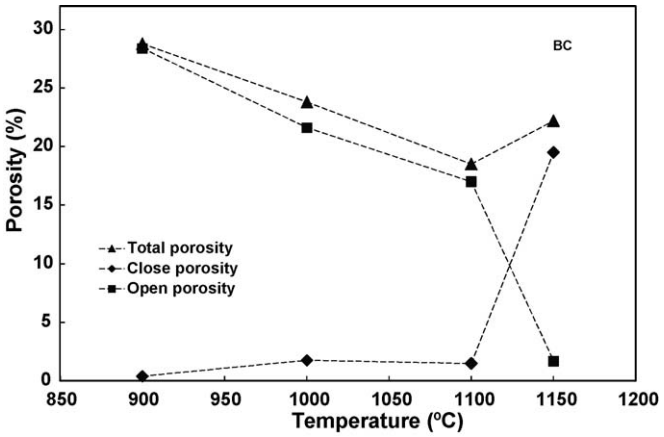

Fig. 6. Total porosity (P_T), close porosity (P_C), and open porosities for He (P_{He}) of the BC samples.

when the crystallization process starts to take place, $\Delta L/Lo$ is only 3%. In the range 1060–1130 °C a secondary sintering process, similar to BG, is observed (Fig. 5) [10].

The dilatometric densification curves of BT, BG and BC, showed that ceramic and glass–ceramic bodies could be obtained via different roots, i.e. by sintering the tuff powder with clays (BC), by sinter-crystallization of the glass frit (BG) or the as it is tuff powder (BT).

The hot-stage microscopy technique confirmed the dilatometric results, showing the beginning of sintering at about 1100 °C and deformation after ∼1200 °C for BC sample. Due to the reduction of Fe^{+3} to Fe^{+2} and gas release, the deformation is accompanied by a volume increase. This phenomenon is common to ceramics with a high percentage of iron oxides [36–38].

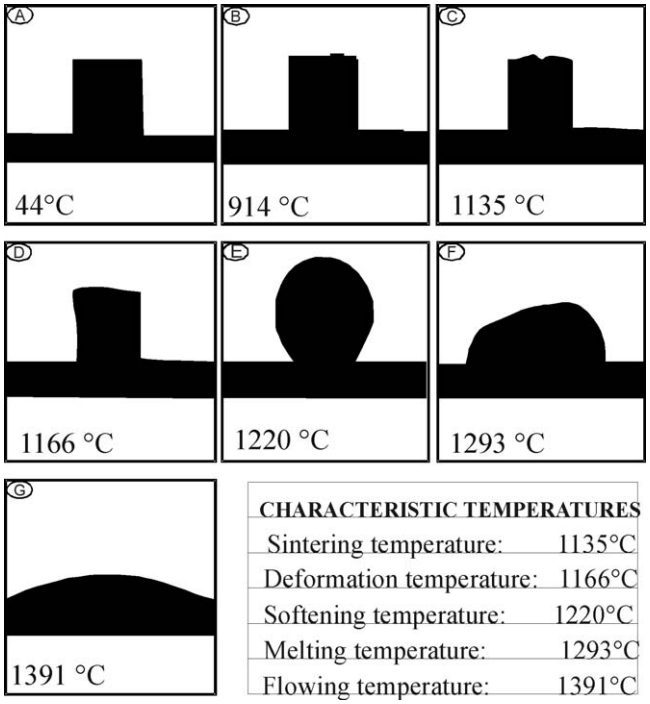

Fig. 5. Hot-stage microscopy analysis of the composition: (A) 44 °C, (B) 914 °C, (C) 1135 °C, (D) 1166 °C, (E) 1220 °C, (F) 1293 °C, and (G) 1391 °C.

These preliminary results supported the choice of carrying out further studies employing the BT and BC samples only.

The densification of BT and BC after isothermal heat-treatment at different temperatures, was estimated by measuring the variation of apparent, ρ_a, skeleton, ρ_s, and absolute, ρ_r, densities. Fig. 6 shows the corresponding total porosity (P_T), close porosity (P_C), and open porosities for He (P_{He}), of the ceramic sample (BC). At 900 °C no significant densification occurs. At 1000 °C and 1100 °C P_T decreases but with a similar closed porosity, P_{He}, value. The almost complete sintering, leading to sample without open porosity, occurs at 1150 °C. The closed porosity of this sample, nevertheless, remains quite high indicating an over-firing process. In order to reduce the over-firing effect, the sintering time at 1150 °C was shortened to 30 min; the obtained W, ρ_a, ρ_s and ρ_r are given in Table 2. Values of 13% total porosity and 4% water absorption, which are typical of earthenware tiles made by a comparable thermal cycle, were obtained. The total porosity (P_T), close porosity (P_C), and open porosities for He (P_{He}) of the sintered basaltic tuff at different temperatures are presented in Fig. 7. Respect to the BC sample at lower sintering temperature, the BT has better densification at 1120 °C with: ∼7% closed and only ∼2% open porosities.

Fig. 8 shows the XRD spectra of the parent BT together with final BC ceramic heated up to 1150 °C and BT-gc and BG-gc glass ceramics heated up to 1100 °C for 1 h,

Table 2
Water absorption, apparent density, skeleton density and absolute density of BC sample at different temperatures.

T (°C)	W % (%)	ρ_a (g/cm^3)	ρ_s (g/cm^3)	ρ_r (g/cm^3)
900(2 h)	13.61 ± 0.06	1.95 ± 0.016	2.73 ± 0.004	2.74 ± 0.003
1000(2 h)	11.19 ± 0.05	2.11 ± 0.014	2.72 ± 0.003	2.77 ± 0.002
1100(2 h)	6.96 ± 0.04	2.24 ± 0.013	2.71 ± 0.004	2.75 ± 0.003
1150(2 h)	0.32 ± 0.05	2.03 ± 0.015	2.14 ± 0.005	2.66 ± 0.002
1150(0.5 h)	3.86 ± 0.04	2.32 ± 0.014	2.61 ± 0.003	2.72 ± 0.003

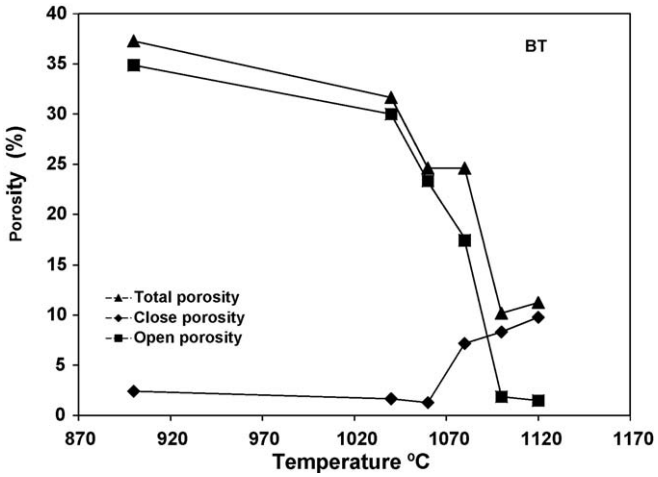

Fig. 7. Total porosity (P_T), closed porosity (P_C) and open porosity for He (P_{He}) of the sintered BT samples.

respectively. The XRD of BT shows elevate amount of amorphous phase (60–70%), clino-pyroxene as a main crystal phase and plagioclases (anorthite solid solution), olivine (forsterite solid solution) and spinels as secondary phases. The XRD analysis of BC show a 30–40% amorphous phase, quartz and anorthite plagioclases as main crystalline phases and ortho-pyroxene, olivine, hematite and spinels as secondary ones. In the BC spectrum, the quartz peaks arises from the clay, the olivine and spinels from the basaltic tuff while the other crystalline phases are formed during the sinter-crystallization process.

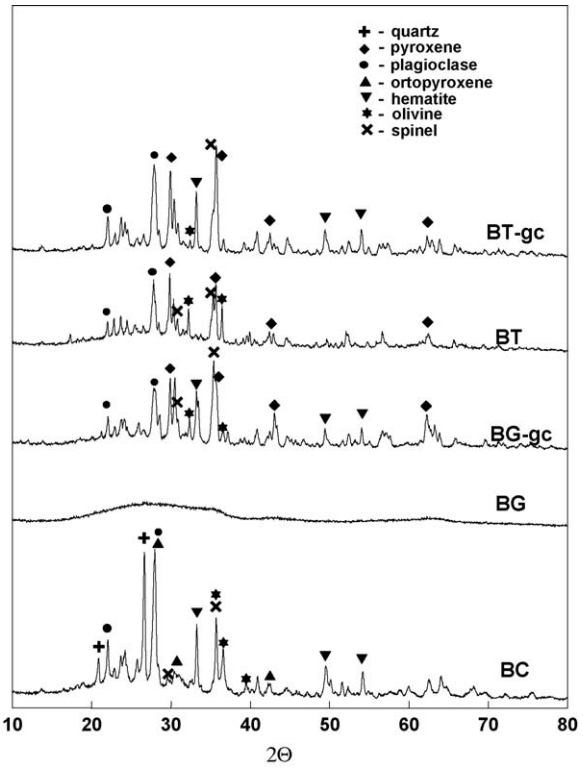

Fig. 8. X-ray spectra of BT, BT-gc, BG-gc, BC and BG.

The BG-gc sample, heated up to 1100 °C has crystallinity of 45 ± 5 wt%, the main crystal phases being spinel, pyroxene, hematite, anorthite plagioclase and olivine. Finally, the SEM observation of the obtained ceramic at 1150 °C and

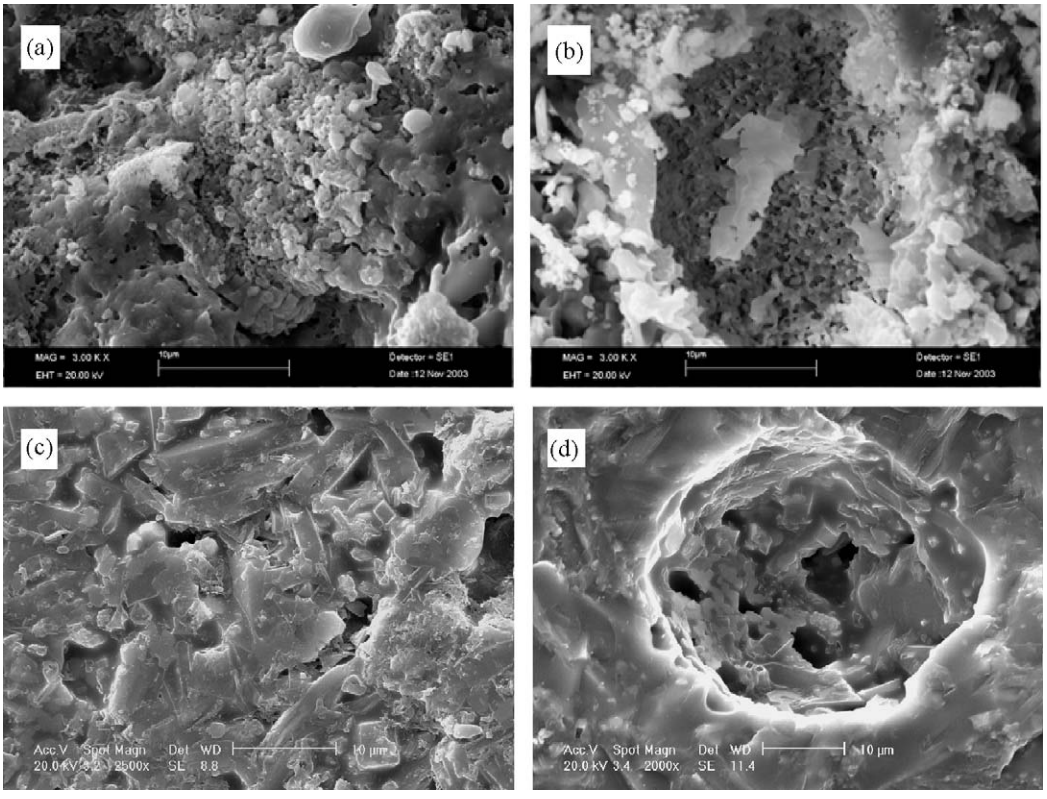

Fig. 9. SEM images of the BC surface (a), fracture (b), BT-gc surface (c) and fracture (d).

glass–ceramic at 1120 °C show the degree of densification in both BC and BG-gc. Fig. 9a and c were taken on the surface of the samples while Fig. 9b and d on the fracture, for BT-gc and BC, respectively. The images confirm the better densification and lower porosity of BT-gc sample, as evaluated by density measurements. The SEM picture of BT-gc surface (Fig. 9c) shows the typical morphology of the pyroxene and hematite crystals.

4. Conclusion

Ceramic material, based on 50% tuffs and 50% clays, with low porosity (13% total) and water absorption (4%) was obtained at 1150 °C. These values are comparable with the commercial earthenware tiles, manufactured by similar production cycle. The ceramic is characterized by a high degree of crystallinity, due to the intensive re-crystallization of plagioclases and ortho-pyroxene.

Glass ceramics were obtained after melting of the tuff at 1350 °C, followed by sinter-crystallization in the range of 1020–1080 °C.

Sintered glass–ceramic materials with higher degree of crystallinity were also produced directly from the milled tuffs, without melting process, after heat-treatment at 1120 °C showing ∼7% closed and only ∼2% open porosities.

The present study has demonstrated that, due to high porosity and low crystallinity, the investigated tuff is suitable for substituting raw materials in the ceramic and glass–ceramic preparation. Further studies are carried out to characterize the physical and mechanical properties of the ceramic and glass–ceramic bodies.

Acknowledgment

The authors wish to thank Prof. Donatello Magaldi for his contribution to the paper preparation by comments and discussions.

References

[1] A. Tucci, L. Esposito, E. Rastelli, C. Palmonari, E. Rambaldi, Use of soda-lime scrap-glass as a fluxing agent in a porcelain stoneware tile mix, Journal of European Ceramic Society 24 (2004) 83–92.
[2] G. Garbonchi, M. Dondi, N. Morandi, F. Tateo, Possible use of altered volcanic ash in ceramic tile production, Industrial Ceramics 19 (1999) 67–74.
[3] F. Matteucci, M. Dondi, G. Guarini, Effect of soda-lime glass on sintering and technological properties of porcelain stoneware tiles, Ceramics International 28 (2002) 873–880.
[4] R. Gennaro, P. Cappelletti, G. Cerri, M. Gennaro, M. Dondi, G. Guarini, A. Langella, D. Naimo, Influence of zeolites on the sintering and technological properties of porcelain stoneware tiles, Journal of European Ceramic Society 23 (2003) 2237–2245.
[5] F. Andreola, L. Barbieri, A. Corradi, I. Lancellotti, T. Manfredini, Utilisation of municipal incinerator grate slag for manufacturing of porcelainized stoneware tiles manufacturing, Journal of European Ceramic Society 22 (2002) 1457–1462.
[6] A. Karamanov, E. Karamanova, A.M. Ferrari, F. Ferrante, M. Pelino, The effect of scrap addition on the sintering behavior of hard porcelain, Ceramics International 32 (2006) 727–732.
[7] M.F. Abadir, E.H. Sallam, I.M. Bakr, Preparation of porcelain tiles from Egyptian raw materials, Ceramics International 28 (2002) 303–310.
[8] K. Dana, S. Das, S.K. Das, Effect of substitution of fly ash for quartz in triaxial kaolin–quartz–feldspar system, Journal of European Ceramic Society 24 (2004) 3169–3175.
[9] P. Torres, H.R. Fernandes, S. Agathopoulos, D.U. Tulyaganov, J.M.F. Ferreira, Incorporation of granite cutting sludge in industrial porcelain tile formulations, Journal of European Ceramic Society 24 (2004) 3177–3185.
[10] S. Ergul, M. Akyildiz, A. Karamanov, Ceramic Material from Basaltic Tuffs, Industrial Ceramics 27 (2) (2007) 89–94.
[11] V. Mangien, D.R. Neuville, L. Cormier, J. Roux, J.L. Hazemann, D. de Lingy, S. Pascarelli, I. Vickridge, O. Pinet, P. Richet, Kinetics and mechanisms of iron redox reactions in silicate melts: the effects of temperature and alkali cations, Geochimica et Cosmochimica Acta 72 (8) (2008) 2157–2168.
[12] H. Beall, H.L. Rittler, Basalt glass ceramics, Ceramic Bulletin 55 (1976) 579–582.
[13] S. Yilmaz, O.T. Ozkan, V. Gunay, Crystallization kinetics of basalt glass, Ceramics International 22 (1996) 477.
[14] G. Bayrak, S. Yilmaz, Crystallization kinetics of plasma sprayed basalt coatings, Ceramics International 32 (2006) 441.
[15] D.J.M. Burkhard, T. Scherer, Surface oxidation of basalt glass/liquid, Journal of Non-Crystalline Solids 352 (2006) 3961.
[16] D. Schreiber, B.K. Kochanowski, C.W. Shreberg, Environmental and waste management issues in the ceramic industry, Ceramic Transactions 39 (1994) 141–149.
[17] A. Karamanov, G. Taglieri, M. Pelino, Iron-rich sintered glass-ceramics from industrial wastes, Journal of American Ceramic Society 82 (1999) 3012–3016.
[18] M. Romero, J.Ma. Rincon, Preparation and properties of high iron oxide content glasses obtained from industrial wastes, Journal of European Ceramic Society 18 (1998) 153–160.
[19] A. Karamanov, M. Pelino, Crystallization phenomena in iron rich glasses, Journal of Non-Crystalline Solids 281 (2001) 139–151.
[20] I. Gutzow, R. Pascova, A. Karamanov, J. Schmelzer, The kinetics of surface induced sinter crystallization and the formation of glass–ceramic materials, Journal of Materials Science 33 (21) (1998) 5265–5273.
[21] Z. Strand, Glass ceramic materials, Glass and Technology, 8, Elseiver, Amsterdam, 1986.
[22] W. Hőland, G. Beall, Glass-Ceramics Technology, The American Ceramics Society, Westerville, 2002.
[23] A. Karamanov, P. Pisciella, C. Cantalini, M. Pelino, The influence of the Fe^{3+}/Fe^{2+} ratio on the crystallization of iron-rich glasses from industrial wastes, Journal of American Ceramic Society 81 (12) (2000) 3153–3157.
[24] P. Pisciella, S. Crisucci, A. Karamanov, M. Pelino, Chemical durability of glasses obtained by vitrification of industrial wastes, Waste Management 21 (2001) 1–9.
[25] A. Karamanov, R. di Gioaccino, P. Pisciella, M. Pelino, Glass transformation range of iron-rich glass and glass-ceramics, Glass Technology 42 (2001) 126–129.
[26] http://www.micromeritics.com.
[27] A. Winchester, P.A. Floyd, Geochemical discrimination of different magma series and their differentiation products using immobile elements, Chemical Geology 20 (1977) 325–343.
[28] S.A. Morse, Basalts and Phase Diagrams, Springler-Verlag, New York, Heidelberg, Berlin, 1982.
[29] A. Karamanov, P. Pisciella, M. Pelino, The crystallisation kinetics of iron rich glass in different atmospheres, Journal of European Ceramic Society 20 (2000) 2233–2237.
[30] A. Karamanov, M. Pelino, Crystallisation phenomena in iron rich glasses, Journal of Non-Crystalline Solids 281 (2001) 139–151.
[31] A. Karamanov, G. Taglieri, M. Pelino, Sintering behavior and properties of iron-rich glass-ceramics, Journal of American Ceramic Society 87 (2004) 1571.
[32] J.Ma. Rincon, M. Pelino, M. Romero, in: Proceedings of the First National Congress Valorization and Recycling of Industrial Wastes, L'Aquila, Italy, July 7–10, (1997), p. 169.

[33] M. Pelino, C. Cantalini, J.Ma. Rincon, Preparation and properties of glass–ceramic materials obtained by recycling goethite industrial waste, Journal of Material Science 32 (1997) 4655–4660.
[34] M.R. James, N. Bagdassarov, K. Muller, H. Pinkerton, Viscoelastic behaviour of basaltic lavas, Journal of Volcanology and Geothermal Research 132 (2004) 99–113.
[35] P.M. Sørensen, M. Pind, Y.Z. Yue, R.D. Rawlings, A.R. Boccaccini, E.R. Nielsen, Effect of the redox state and concentration of iron on the crystallization behavior of iron-rich aluminosilicate glasses, Journal of Non-Crystalline Solids 351 (2005) 1246–1253.
[36] W.D. Kingery, Introduction to Ceramics, J. Wiley & Sons, New York, 1976.
[37] J.S. Reed, Principles of Ceramic Proceedings, J. Wiley & Sons, New York, 1995.
[38] J. Hlavac, The Technology of Glass and Ceramics: an Introduction, Elsevier, Amsterdam, 1983.